$$a_1 = 0{,}027, \quad b_1 = 0{,}025, \quad c_1 = 0{,}025,$$
$$a_2 = -0{,}13, \quad b_2 = -2{,}0, \quad c_2 = -2{,}85,$$
$$a_3 = -5{,}60, \quad b_3 = -2{,}0, \quad c_3 = -3{,}80,$$
$$l_1 = 0{,}11, \quad l_2 = -0{,}333, \quad l_3 = -4{,}52,$$
$$m_1 = 0{,}115, \quad m_2 = -2{,}0, \quad m_3 = -2{,}0.$$

3. The time to calculate a single variant is 6-10 min on a BÉSM-6 computer with grid steps $h_x = h_y = 0.1$.

4. The calculated and experimental values of the mean-temperature defect (Fig. 1) for jet cross sections $\hat{x} = 40$-80 diameters are in agreement within the limits of physical error of the measurements (3-8%). The error increases as the cross section approaches the nozzle. When $\hat{x} = 20$, it is 15%.

5. The calculational and experimental results of the transverse heat flux (Fig. 2) agree within the limits of physical error of the measurements close to the axis, but give a relative error of the order of 50% close to the boundary. When $\xi_t \leq 0.8$, the normalized flux is smaller for smaller cross sections; when $\xi_t \geq 1.0$, the opposite is true.

6. The normalized mean-square temperature pulsations (Fig. 3) agree with experiment within the limits of physical error of the measuremens. The maximum value of the normalized pulsations increaseswith increase in distance from the nozzle. The greatest deviation from experiment is observed at distances $\hat{x} = 20$-30 diameters from the nozzle.

7. The variation in dissipation rate of the temperature pulsations is shown in Fig. 4. The lack of experimental data prevents a comparison.

LITERATURE CITED

1. R. A. Antonia, Int. J. Heat Mass Transfer, 28, No. 10, 1805-1812 (1985).
2. B. E. Launder, Topics in Applied Physics, Springer, Berlin (1976), pp. 231-287.
3. E. V. Radkevich, in: Application of Mathematical Methods and Computational Techniques in Solving Economic Problems [in Russian], Gomel' (1986), p. 255.
4. V. N. Abrashin, V. N. Barykin, and E. V. Radkevich, Algorithm and Some Results of Calculating Plane Isothermal Gas Jet. Preprint No. 22 [in Russian], Institute of Mathematics, Academy of Sciences of the Belorussian SSR, Minsk (1986).

INFLUENCE OF THE VELOCITY PROFILE ON THE HEAT TRANSFER OF A CIRCULAR IMPACT JET

A. I. Abrosimov and A. V. Voronkevich

UDC 536.242:532.525.2

The influence of the mean velocity profile in a round submerged jet on the heat transfer with a plane obstacle placed along the normal to the flow is investigated. A criterial relation for the heat transfer in the vicinity of the critical point is obtained.

The interaction of an immersed impact jet with a uniform velocity profile at the nozzle outlet and a low level of initial turbulence ε_0 with an obstacle is characterized by maximum effectiveness of heat transfer at a distance of $h = 7$-8 in the vicinity of the critical point of the obstacle [1]. This has been noted in many works. In [2], it was suggested that the presence of a peak of the heat-transfer coefficient in the vicinity of the critical point is a result of the combined influence of increase in intensity of turbulence at the jet axis ε_m and decrease in the axial velocity in the transitional section of the jet.

All-Union Scientific-Reserach Institute of Electromechanics, Istra. Translated from Inzhenerno-Fizicheskii Zhurnal, Vol. 54, No. 3, pp. 393-398, March, 1988. Original article submitted November 12, 1986.

0022-0841/88/5403-0262$12.50

However, in the given range of h, scattering of a free submerged jet is accompanied not by increase in ε_m but by continuous deformation of the velocity profile. The velocity distribution in the initial and transitional sections of the jet is not self-similar, and rearrangement of the profile in the transitional section is accompanied by decrease in axial velocity.

In [3, 4], for plane and circular laminar in impact jets, respectively, significant influence of the velocity profile on the heat transfer was observed. Thus, transition from a rectangular initial velocity profile to a parabolic profile at a distance h = 2 is accompanied by increase in heat-transfer coefficient at the critical point by a factor of approximately two [4].

An impact jet is usually represented as consisting of a region of flow developing according to the law of a free immersed jet and an interaction region, which begins at the cross section where the decrease in axial velocity under the influence of a plate placed transverse to the flow becomes pronounced.

The flow in the interaction region is assumed to be laminar.

Integration of the complete Navier–Stokes and energy equaitons is undertaken for the interaction region. The liquid is assumed to be incompressible and the thermophysical properties to be constant. The equation is solved numerically by the finite-difference method described in [5]. The calculation region is bounded by the obstacle, the plane of onset of the interaction at a distance

$$x_p = 1 + 0{,}05h, \tag{1}$$

from the obstacle, and a cylindrical surface of radius

$$r_p = 2 + 0{,}1h. \tag{2}$$

The specification of the boundary conditions at the obstacle, the cylindrical surface, and the part of the plane of onset of interaction not occupied by the incoming jet and also the calculation of vorticity at the wall and the axis are as in [5]. The temperature distribution at the obstacle is assumed to be uniform. The mean-velocity profile in the free jet is determined using a P function [6]

$$\frac{v}{v_{m_0}} = \frac{1}{\sigma_v^2}\exp\left(-\frac{r^2}{2\sigma_v^2}\right)\int_0^{r_0}\exp\left(-\frac{\rho^2}{2\sigma_v^2}\right)I_0\left(\frac{r\rho}{\sigma_v^2}\right)\rho d\rho, \tag{3}$$

where I_0 is a zero-order Bessel-function of an imaginary argument; σ_v is the mean square radius of the mean-velocity profile, $\sigma_v/\sqrt{2}r_0 = \sqrt{\xi}/r_0$; v_{m_0} is the velocity at the axis in the initial cross section of the jet; P is a function tabulated in [7]. Using Eq. (3), the continuous deformation of the velocity profile from the initial — for example, rectangular — form to a Gaussian form far downstream.

At the end of the initial section of the jet, $\sqrt{\xi}/r_0 = 0.18$. In the region $1 \leq h_p \leq h_{in}$, the variation in $\sqrt{\xi}/r_0$ is represented by the approximate dependence [6]

$$\frac{\sqrt{\xi}}{r_0} = 0{,}18h_p/h_{in}, \text{ where } h_p = h - x_p. \tag{4}$$

In the transitional and basic sections of the jet, $\sqrt{\xi}/r_0$ is determined from the table of P functions using experimental data on the scattering of the axial velocity.

The conditions of outflow of the given jets and the values of the axial velocity at the input to the calculation region for the specified distances between the nozzle outlet and the barrier are shown in Table 1.

The velocity value for each point of the calculation grid at the input to the interaction region isdetermined from the value of $\sqrt{\xi}/r_0$ obtained and the table of P functions. The calculation grid (23 × 23 points) is denser close to the wall and in the radial direction close to r = 0.5. Inside the wall boundary layer there are 7-9 points of the grid distributed according to a geometric progression. Preliminary calculations show that the thickness of the wall boundary layer close to the axis is $\delta_m \sim Re^{-0.38}$. The distance from the wall to the closest point varies in proportion to δ and is $7\cdot10^{-4}$ d for Re = 21,000, for example. The calculation point closest to the axis lies at a distance of 0.1 d. The criterion of convergence of the difference problem is taken to be

TABLE 1. Initial Intensity of Turbulence at the Nozzle Outlet and Axial-Velocity Values at the Input to the Calculation Region

Initial velocity profile	ε_0	$(v_m/v_{m_0})_p$					Lit. source
		$h=2$	$h=4$	$h=6,3$	$h=8$	$h=10$	
Rectangular	0,01	1	1	1	0,95	0,83	[8]
Rectangular	0,093	1	0,982	0,741	0,59	0,511	[8]
Rectangular	0,209	0,89	0,662	0,524	0,457	0,408	[8]
Developed turbulent	0,02	1	0,991	0,949	0,854	0,709	[9]
Parabolic laminar jet	—	0,999	0,998	0,996	0,995	0,993	[10]

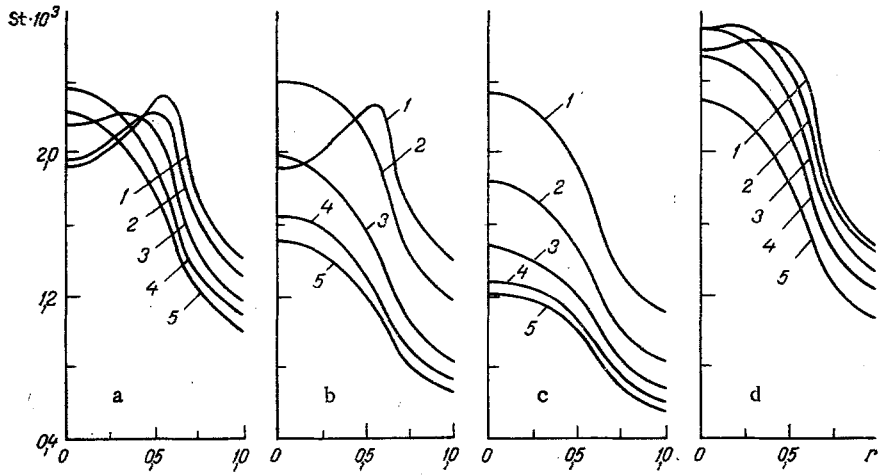

Fig. 1. Variation in local heat transfer along obstacle (Re = 11,000, Pr = 9.6): a, b, c) rectangular initial velocity profile; ε_0 = 0.01 (a), 0.093 (b), 0.209 (c); d) developed turbulent initial velocity profile, ε_0 = 0.02; h = 2 (1), 4 (2), 6.3 (3), 8 (4), and 10 (5).

$$\left(\frac{f^n - f^{n-1}}{f_{\max}^{n-1}}\right)_{\max} \leqslant 10^{-3},$$

where f is variable; n is the number of iterations, the subscript max denotes the greatest value in the field of the variables.

The radial distribution of local heat-transfer coefficients under various conditions of jet emission and at various distances h is shown in Fig. 1. If the jet has a uniform velocity profile in the initial cross section and $\varepsilon_0 \leq 0.01$ (Fig. 1a), then the maximum heat-transfer intensity when h = 2 is found not at the critical point but is shifted from the axis by approximately 0.55 d. Up to r = 0.8, values of the number St obtained are in satisfactory agreement with experiment [1]. The reasons for the appearance of a peak in the distribution of St were considered in [4]. With increase in the distance between the obstacle and the nozzle, the peak is shifted toward the axis, and decreases slightly in magnitude. At a distance h = 6.3, the peak becomes almost imperceptible. Beginning at a distance h = 8, the distribution takes on a bell-like form, with the maximum of heat-transfer intensity in the vicinity of the critical point.

With increase in initial intensity of the turbulence, rearrangement of the jet velocity profile from rectangular form to self-similar form occurs more rapidly. Therefore, for a jet with ε_0 = 0.093 (Fig. 1b), the internal peak occurs only at a distance h = 2, and at $h \geq 4$ the distribution of St is characterized by smooth decrease with increasing distance from the critical point. Calculation shows that, when ε_0 = 0.209, even at h = 2, the curve of variation in the heat-transfer coefficient has the usual bell-like form with a maximum close to the critical point (Fig. 1c).

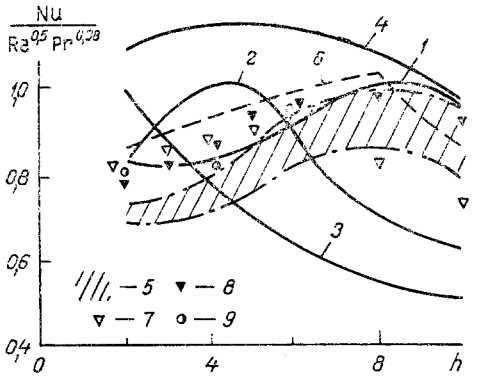

Fig. 2

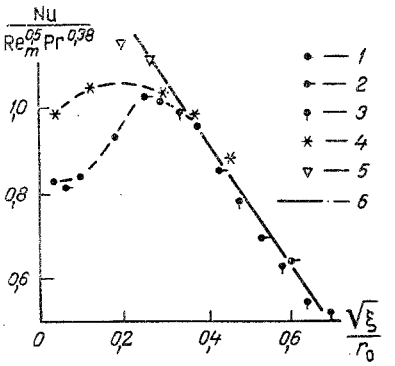

Fig. 3

Fig. 2. Dependence of the heat-transfer coefficient in the vicinity of the critical point on the conditions of jet emission and on h: 1-3) rectangular initial velocity profile with ε_0 = 0.01 (1), 0.093 (2), 0.209 (3); 4) developed turbulent initial velocity profile, ε_0 = 0.02; 5-9) rectangular initial velocity profile, $\varepsilon_0 \leq$ 0.01; 5) Re = (0.7-11.2)•10^4, experiment [1]; 6) empirical relations [13]; 7) Re = 3.24•10^4, experiment [11]; 8) Re = 1.48•10^5, experiment [11]; 9) Re = 6.6•10^4, experiment [14].

Fig. 3. Heat transfer in the vicinity of the critical point of a barrier: 1-3) rectangular initial velocity profile; ε_0 = 0.01 (1), 0.093 (2), 0.209 (3); 4) developed turbulent initial velocity profile, ε_0 = 0.02; 5) laminar jet with parabolic initial velocity profile; 6) Eq. (6).

For a jet with developed turbulent initial velocity profile and ε_0 = 0.02, the presence of a peak (admittedly small) in the heat-transfer intensity at r = 0.35 is seen (Fig. 1d). At h = 4, the peripheral peak is again not observed.

The variation in heat-transfer coefficient in the vicinity of the critical point of the obstacle immersed in impact jets with different emission conditions is shown in Fig. 2. With a rectangular initial velocity profile and ε_0 = 0.01, the heat-transfer intensity smoothly increases to approximately h = 8.5 with increasing distance between the nozzle and obstacle (starting from h = 2) and then begins to decrease. Note that at h = 2 the data obtained are in best agreement with calculations by the formula in [12]

$$\mathrm{Nu} = 0{,}763\,(\beta_{u_m}\mathrm{Re})^{0,5}\mathrm{Pr}^{0,39}. \qquad (5)$$

Experimental data of various authors are also shown in Fig. 2. The qualitative agreement of calculation and experiment is satisfactory. Note that continuous deformation of the jet velocity profile at the input to the interaction region is taken into account in obtaining the present results, and it is also assumed that there is no turbulent transfer in this region. Therefore, it may be concluded that the maximum of the curve Nu = f(h) is due not only to increase in the intensity of turbulence ε_m and decrease in the velocity at the axis in the transitional section but also to deformation of the velocity profile in cross sections of the flux at the input to the unreaction interaction region with variation in h. In view of the considerable scatter of experimental data, additional investigations are required to elucidate the influence of each factor separately.

It may be assumed that the relation Nu ~ $\mathrm{Re}^{0.5}$ when $\delta_m \sim \mathrm{Re}^{-0.38}$ is due to the structural features of the wall boundary layer in its external section.

With increase in the initial intensity of the turbulence, while retaining uniform velocity profile at the nozzle outlet, the maximum of the heat transfer at the critical point is shifted to smaller h. For example, if ε_0 = 0.093 (Fig. 2, curve 2), the maximum of the heat transfer is approximately at a distance h = 4.4. It is characteristic that, when ε_0 = 0.209, no maximum is observed in the distribution of the heat-transfer coefficient. The transition from a rectangular profile to a developed turbulent profile (Fig. 2, curve 4) leads to intensification of heat transfer in the given range of h. The maximum in the distribution Nu = f(h) is also present here, at a distance h = 5. Further increase in heat-transfer intensity is seen on passing to a parabolic initial velocity profile. In this case, the heat-transfer intensity in the vicinity of the critical point decreases monotonically with increase in h.

Analysis of the data obtained shows (Fig. 3) that, in the range $0.3 \leq \sqrt{\xi}/r_0 \leq 0.7$, the heat transfer in the vicinity of the critical point for all the given conditions is described by the following relation, with an error no greater than 7%

$$\mathrm{Nu} = \left(1{,}51 - 0{,}45\frac{\sqrt{\xi}}{r_0}\right)\mathrm{Re}_m^{0{,}5}\mathrm{Pr}^{0{,}38}. \qquad (6)$$

For laminar and turbulent flow, without taking account of the turbulent mechanism of heat transfer in the region of interaction of isothermal jets, the heat transfer in the vicinity of the critical point may be written in the form of a single dependence on $\sqrt{\xi}/r_0$. Equation (6) gives values of the heat-transfer coefficient close to the experimental results.

In the region $0.03 \leq \sqrt{\xi}/r_0 < 0.3$, the heat-transfer intensity in the vicinity of the critical point increases with increase in nonuniformity of the velocity distribution in the initial cross section of the jet. The dependence $\mathrm{Nu}/\mathrm{Re}_m^{0.5}\,\mathrm{Pr}^{0.38} = f(\sqrt{\xi}/r_0)$ retains its form for jets with a rectangular initial velocity profile and different intensities of turbulence at the nozzle outlet.

NOTATION

d, nozzle diameter; $x = X/d$, $r = R/d$, dimensionless coordinates directed along the jet axis and the normal to the axis, respectively; $h = H/d$, dimensionless distance from the nozzle outlet to the obstacle; V_0, mean mass velocity at the nozzle outlet; x_p, dimensionless height of calculation region; r_p, dimensionless radius of calculation region; $v = V/V_0$, $u = U/V_0$, dimensionless velocity components with respect to the x and r coordinates, respectively; $\mathrm{Re} = V_0 d/\nu$, $\mathrm{Re}_m = v_{m_0} d/\nu$, Reynolds numbers; $\mathrm{St} = \alpha/\rho c_p V_0$, Stanton number; $\mathrm{Pr} = \nu c_p \rho/\lambda$, Prandtl number; $\mathrm{Nu} = \alpha d/\lambda$, Nusselt number; δ_m, thickness of wall boundary layer close to axis βu_m, dimensionless radial-velocity gradient in the vicinity of the critical point; $\varepsilon = \sqrt{v'^2}/v$, intensity of turbulence. Indices: m, parameters at external boundary of wall boundary layer and at jet axis; 0, parameters at nozzle outlet.

LITERATURE CITED

1. R. Gardon and J. Cobonpue, in: International Developments in Heat Transfer: Proceedings of International Heat Transfer Conference, American Society of Mechanical Engineers, New York (1961), pp. 454-460.
2. R. Gardon and J. Akfirat, Int. J. Heat Mass Transfer, 8, No. 10, 1261-1272 (1965).
3. E. M. Sperrow and L. Li, Trans. ASME, Ser. C [Russian translation], 97, No. 2, 34-42 (1975).
4. A. I. Abrosimov, Teplofiz. Vys. Temp., 22, No. 3, 512-516 (1984).
5. A. D. Gosmen, V. M. Pan, A. K. Ranchel, et al., Numerical Methods of Investigating the Flow of Viscous Liquid [in Russian], Moscow (1972).
6. A. G. Prudnikov, M. S. Volynskii, and V. N. Sagalovich, Mixture Formation and Combustion in Air-Reactive Motors [in Russian], Moscow (1971).
7. L. A. Vulis, Sh. A. Ershin, and L. P. Yarin, Fundamentals of Gas-Flame Theory [in Russian], Moscow (1968).
8. G. S. Ginevskii, Theory of Turbulent Jets and Wakes [in Russian], Moscow (1969).
9. R. Wille, Z. Flugwiss., No. 6, 222-233 (1963).
10. G. W. Rankin and K. Sridhar, Trans. ASME, J. Fluid. Eng., 103, No. 6, 322-327 (1981).
11. E. P. Dyban and A. I. Mazur, Teplofiz. Teplotekh., No. 33, 6-10 (1977).
12. M. Sibulkin, J. Aeronaut. Sci., 19, No. 2, 570-571 (1952).
13. E. P. Dyban and A. I. Mazur, Convective Heat Transfer with Jet Flow around Bodies [in Russian], Kiev (1982).
14. C. J. Hoogendoorn, Int. J. Heat Mass Transfer., 20, No. 12, 1333-1338 (1977).